Coxiella burnetii effector protein subverts clathrin-mediated vesicular trafficking for pathogen vacuole biogenesis

Charles L. Larson, Paul A. Beare, Dale Howe, and Robert A. Heinzen[1]

Coxiella Pathogenesis Section, Laboratory of Intracellular Parasites, Rocky Mountain Laboratories, National Institute of Allergy and Infectious Diseases, National Institutes of Health, Hamilton, MT 59840

Edited by Yasuko Rikihisa, The Ohio State University, Columbus, OH, and approved October 25, 2013 (received for review May 14, 2013)

Successful macrophage colonization by *Coxiella burnetii*, the cause of human Q fever, requires pathogen-directed biogenesis of a large, growth-permissive parasitophorous vacuole (PV) with phagolysosomal characteristics. The vesicular trafficking pathways co-opted by *C. burnetii* for PV development are poorly defined; however, it is predicted that effector proteins delivered to the cytosol by a defective in organelle trafficking/intracellular multiplication (Dot/Icm) type 4B secretion system are required for membrane recruitment. Here, we describe involvement of clathrin-mediated vesicular trafficking in PV generation and the engagement of this pathway by the *C. burnetii* type 4B secretion system substrate *Coxiella* vacuolar protein A (CvpA). CvpA contains multiple dileucine [DERQ]XXXL[LI] and tyrosine (YXXΦ)-based endocytic sorting motifs like those recognized by the clathrin adaptor protein (AP) complexes AP1, AP2, and AP3. A *C. burnetii* Δ*cvpA* mutant exhibited significant defects in replication and PV development, confirming the importance of CvpA in infection. Ectopically expressed mCherry-CvpA localized to tubular and vesicular domains of pericentrosomal recycling endosomes positive for Rab11 and transferrin receptor, and CvpA membrane interactions were lost upon mutation of endocytic sorting motifs. Consistent with CvpA engagement of the endocytic recycling system, ectopic expression reduced uptake of transferrin. In pull-down assays, peptides containing CvpA-sorting motifs and full-length CvpA interacted with AP2 subunits and clathrin heavy chain. Furthermore, depletion of AP2 or clathrin by siRNA treatment significantly inhibited *C. burnetii* replication. Thus, our results reveal the importance of clathrin-coated vesicle trafficking in *C. burnetii* infection and define a role for CvpA in subverting these transport mechanisms.

type IV secretion | vesicular fusion

The Gram-negative bacterium *Coxiella burnetii* is the causative agent of the zoonosis Q fever, a disease that typically manifests in humans as an acute influenza-like illness. Transmission of the pathogen to humans is linked to inhalation of organisms shed into the environment in large numbers by animal reservoirs. *C. burnetii* initially targets aveolar macrophages and can spread from the lung to colonize mononuclear phagocytes of other tissues. Aerosol transmission, high infectivity, environmental stability, and the debilitating nature of Q fever collectively account for designation of *C. burnetii* as a category B biothreat (1, 2).

Intracellular bacteria that occupy host-derived vacuoles actively modify the compartment to avoid host defenses and generate a growth-permissive intracellular niche (3). Examples include *Legionella pneumophila,* a close relative of *C. burnetii*, that escapes default endocytic trafficking to reside within a vacuole with characteristics of the endoplasmic reticulum (ER) (4). Like other intracellular bacteria, *C. burnetii* actively modifies its intracellular niche, or parasitophorous vacuole (PV). Bacterial protein synthesis is required for homotypic and heterotypic fusion of the PV with cellular vesicles to result in a replication compartment that can occupy nearly the entire host-cell cytoplasm (5–8). However, the *C. burnetii* PV is unique among bacteria-occupied vacuoles by resembling, in structure and function, a large phagolysosome (2). PV maturation in macrophages culminates in acquisition of the endolysosomal proteins Rab7, lysosomal-associated membrane protein 1 (LAMP1), CD63, active cathepsins, and a pH of ∼4.8 (9, 10). Indeed, *C. burnetii* requires the acidic pH of the PV for metabolic activation and replication (11, 12) and resists degradative conditions that quickly destroy *Escherichia coli* (10).

Bacterial pathogens commonly deploy specialized secretion systems to deliver effector proteins directly to the host-cell cytosol that modulate host factors required for pathogen vacuole formation and other infection events (13). *C. burnetii* encodes a Dot/Icm type 4B secretion system (T4BSS) homologous to the T4BSS of *L. pneumophila* (14). Recent advances in *C. burnetii* host-cell–free culture (12) and genetic manipulation (15) have enabled confirmation that type 4B secretion is essential for productive infection. *Himar1* transposon mutagenesis revealed that *icmL* and *icmD* are required for translocation of effectors and colonization of host cells (16, 17). More recently, targeted gene deletion demonstrated the same phenotypes for *C. burnetii* strains missing *dotA* or *dotB* (15).

To date, over 80 *C. burnetii* genes that encode T4BSS substrates have been identified (17–23). These substrates have largely been identified using *L. pneumophila* as a surrogate host and adenylate cyclase or β-lactamase–based translocation assays. Among the large cohort of *C. burnetii* effectors, only three have known functions, all associated with anti-apoptotic activity. The ankyrin repeat-containing protein AnkG inhibits apoptosis by binding the proapoptotic protein p32 (gClqR) (20). *C. burnetii* anti-apoptotic effector B (CaeB) blocks apoptotic signals emanating

Significance

The vesicular trafficking pathways required for generation of the phagolysosome-like vacuole occupied by *Coxiella burnetii* are poorly defined, and no pathogen effectors of vesicular trafficking are known. Here, we reveal an important role for clathrin-mediated vesicular trafficking in *Coxiella* vacuole formation and identify a type 4B secretion system effector protein [*Coxiella* vacuolar protein A (CvpA)] that engages this pathway. *C. burnetii* CvpA traffics through the endocytic recycling compartment, and endocytic sorting motifs within CvpA bind the clathrin adaptor complex AP2. Mutation of *cvpA*, or depletion of AP2 or clathrin, significantly restricts *Coxiella* replication. Thus, our results reveal a effector–clathrin interaction that benefits pathogen replication.

Author contributions: C.L.L., P.A.B., and R.A.H. designed research; C.L.L. and D.H. performed research; C.L.L. and P.A.B. contributed new reagents/analytic tools; C.L.L. and R.A.H. analyzed data; and C.L.L. and R.A.H. wrote the paper.

The authors declare no conflict of interest.

This article is a PNAS Direct Submission.

[1]To whom correspondence should be addressed. E-mail: rheinzen@niaid.nih.gov.

This article contains supporting information online at www.pnas.org/lookup/suppl/doi:10.1073/pnas.1309195110/-/DCSupplemental.

from the mitochondria whereas CaeA inhibits apoptosis by an unknown mechanism (24).

The functional redundancy of effectors that inhibit apoptosis strongly suggests that maintenance of host-cell viability is critical for *C. burnetii* to complete its lengthy infectious cycle (6). However, *C. burnetii* modulation of PV fusogenicity is also considered essential for successful infection. Cell culture infection models have revealed several host vesicular pathways involved in PV biogenesis (5, 7, 25). Disruption of Rab GTPases that regulate endocytic (Rab5 and Rab7), secretory (Rab1), and autophagic (Rab24) vesicular trafficking events produce defects in intracellular replication (5, 8, 26, 27), implying that *C. burnetii* obtains lipids and proteins for PV biogenesis, as well as nutrients for growth, from heterotypic fusion with multiple vesicular compartments. PV fusogenicity is at least partially a consequence of recruitment of soluble *N*-ethylmaleimide-sensitive factor attachment protein receptors (SNAREs). The t-SNARE syntaxin-8 and vesicle-associated membrane protein 7 (VAMP7) localize to the PV membrane (5, 28). Depletion of VAMP7 by siRNA decreases PV size, and expression of a truncated form inhibits homotypic and heterotypic fusion events (5). In a genome-wide siRNA screen, McDonough et al. (25) reported that knockdown of syntaxin-17 also inhibits PV fusion. Thus, *C. burnetii* relies upon multiple SNAREs to promote favorable fusion events. McDonough and coauthors (25) also found a role for retromer-dependent retrieval of receptors from the endolysosomal system based on defects in PV expansion in response to knockdown of retromer subunits (VPS29 and VPS35) or associated sorting nexins (SNX2, SNX3, SNX5, and SNX6).

The complex vesicular interactions that provide membrane for PV expansion are likely regulated by the activities of *C. burnetii* T4BSS effector proteins. A common trait among secreted bacterial effectors is the presence of eukaryotic-like motifs/domains that functionally mimic the activity of host proteins for the benefit of the pathogen (4, 13). A search of the *C. burnetii* genome revealed a gene encoding a predicted protein (CBU0665) with characteristics of a Dot/Icm T4BSS substrate harboring a eukaryotic-like protein–protein interaction domain and multiple endocytic sorting motifs similar to those bound by the heterotetrameric clathrin adaptor protein (AP) complexes AP1, AP2, and AP3. Binding of AP complexes to sorting motifs within the cytoplasmic tails of transmembrane proteins regulates their packaging into clathrin-coated vesicles (CCVs) (29–31). AP1 and AP3 operate as cargo adaptors for the *trans*-Golgi network (TGN)-to-endosome transport, and AP2 mediates plasma membrane-to-endosome transport (29). Given that proteins required for lysosomal biogenesis are delivered by CCVs (32, 33), the endocytic sorting motifs within CBU0665 suggest that it might target clathrin-mediated vesicular trafficking.

Here, we demonstrate that clathrin-mediated transport promotes *C. burnetii* infection and that CBU0665 is a T4BSS effector protein that engages this pathway. Furthermore, using methods for targeted gene inactivation, we establish that CBU0665 function is required for generation of the vacuolar niche of *C. burnetii* and for robust growth of the pathogen in human macrophages.

Results

CBU0665 (CvpA) Is a Dot/Icm T4BSS Substrate. Bioinformatics analysis of the *C. burnetii* Nine Mile RSA493 genome (34) revealed a previously uncharacterized ORF CBU0665, now designated ***C**oxiella **v**acuolar **p**rotein **A*** (*cvpA*), encoding a predicted protein with features of known *C. burnetii* T4BSS effector proteins. First, CvpA contains a eukaryotic-like leucine-rich repeat (LRR) associated with protein–protein interactions (4, 13) and multiple endocytic sorting motifs ([DERQ]XXXL[LI] and YXXΦ, Φ-bulky hydrophobic) like those recognized by the tetrameric clathrin adaptor complexes AP1, AP2, and AP3 (Fig. 1*A*) (29, 31). Second, the C terminus of CvpA contains a distribution of charged and hydrophobic amino acids reminiscent of a characterized Dot/Icm T4B secretion signal (19, 22, 35) (Fig. 1*B*). Third, *cvpA* contains a previously described upstream PmrA regulatory element (18, 36).

T4BSS-dependent delivery of CvpA to the host-cell cytosol was examined using the adenylate cyclase (CyaA) translocation assay (16). Lysates from THP-1 macrophages infected with *C. burnetii* expressing CyaA-CvpA contained ≥50-fold more cAMP than cells infected with bacteria expressing CyaA alone (Fig. 2*A*). No increase in cAMP concentration was detected in cells infected with a *C. burnetii dotA* mutant expressing CyaA-CvpA, confirming T4BSS-dependent translocation of CvpA into the host-cell cytosol.

CvpA Is Required for Replication of *C. burnetii* in Human Macrophages. To examine the importance of CvpA for productive infection of host cells, a Δ*cvpA* mutant was generated and growth was assessed in THP-1 human macrophages (15, 16). Growth of wild-type *C. burnetii* and the Δ*cvpA* mutant was indistinguishable in the axenic medium, ACCM-2 (Fig. 2*B*). However, *C. burnetii* Δ*cvpA* replication was significantly reduced in THP-1 cells at 5 d post infection, as shown by a 14-fold increase in genomic equivalents (GE), relative to a 114-fold increase for wild-type *C. burnetii* (Fig. 2*B*). Impaired growth of *C. burnetii* Δ*cvpA* in THP-1 cells correlated with generation of small, tight-fitting LAMP1-positive vacuoles in Vero cells (Fig. 2 *C* and *D*). Complementation of *C. burnetii* Δ*cvpA* by Tn7::*cvpA* rescued both intracellular replication and PV biogenesis, confirming that the altered phenotypes were due to the absence of CvpA (Fig. 2 *B–D*). These data indicate that CvpA is a Dot/Icm T4BSS effector critical for intracellular growth of *C. burnetii.*

CvpA Traffics Within the Endocytic Recycling Compartment and Localizes to the PV Membrane. The presence of predicted endocytic sorting motifs in CvpA, and the severe growth defect associated with *cvpA* deletion, suggest that the protein engages endocytic vesicles required for PV maturation. CvpA was fused to mCherry and ectopically expressed in HeLa cells, and then trafficking dynamics and colocalization with cellular proteins was examined (Table 1). When live cells were viewed by fluorescence microscopy, mCherry-CvpA labeled the plasma membrane, trafficked dynamically through peripheral tubular vesicles, and

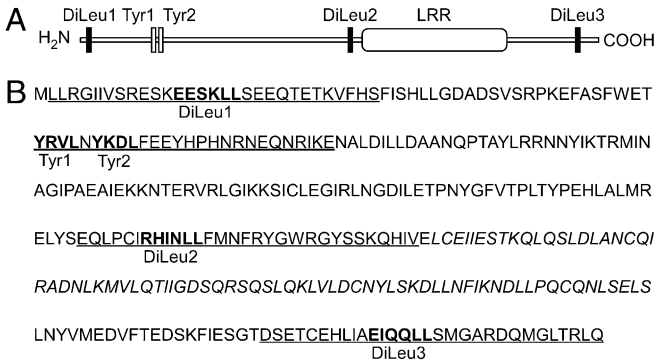

Fig. 1. *C. burnetii* CvpA (CBU0665) contains a eukaryotic-like LRR domain and multiple endocytic sorting motifs. (*A*) Schematic of CvpA (328 aa, 38.0 kDa) showing the LRR and distribution of dileucine (DiLeu) and tyrosine (Tyr) endocytic sorting motifs identified using the Eukaryotic Linear Motif resource for functional sites in proteins (www.ELM.eu.org). (*B*) CvpA amino acid sequence. Consensus dileucine [DERQ]XXXL[LI] and tyrosine (YXXΦ; Φ, amino acid with a bulky hydrophobic side chain) endocytic sorting motifs are shown in boldface type. The amino acid sequence of peptides used in GST-30mer pull-down assays are underlined, and the LRR sequence is italicized.

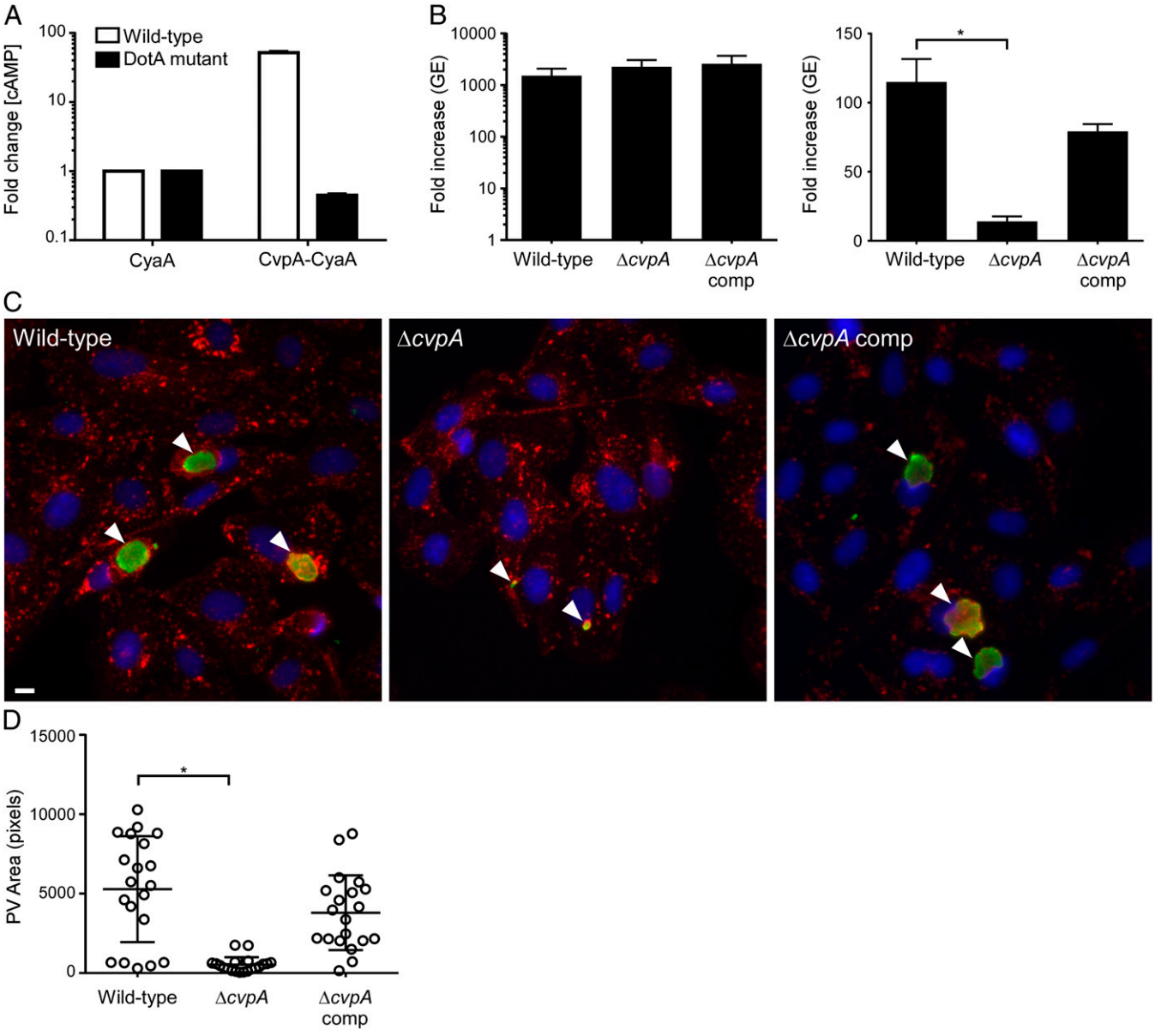

Fig. 2. CvpA is a Dot/Icm T4BSS substrate required for intracellular growth of *C. burnetii*. (*A*) Production of cytosolic cAMP by THP-1 cells infected with *C. burnetii* expressing CyaA-CvpA (*Left*). Cell lysates were collected 48 h post infection (pi), and fold increases in cAMP were determined relative to lysates from cells infected with *C. burnetii* expressing CyaA alone. Values are mean ± SEM of duplicate samples and are representative of three independent experiments. (*B*) Replication of wild-type *C. burnetii*, the Δ*cvpA* mutant, and the complemented mutant in ACCM-2 (*Left*) and THP-1 macrophages (*Right*). Fold increases in GEs at 5 d pi are depicted. Results are expressed as the means of two biological replicates representative of three independent experiments. Error bars indicate SE from the means, and an asterisk indicates a statistically significant difference ($P < 0.05$). (*C*) Representative epifluorescent micrographs of Vero cells infected with wild-type *C. burnetii*, the Δ*cvpA* mutant, or the complemented mutant. Vero cells were infected for 5 d and then immunostained for LAMP1 (red), *Coxiella* (green), and DNA (blue). Arrowheads denote PVs. (Scale bar, 10 μm.) (*D*) Size of PVs generated by wild-type *C. burnetii*, the Δ*cvpA* mutant, and the complemented mutant after 5 d growth in Vero cells as measured using ImageJ ($n = 20$). Error bars indicate SE from the means, and the asterisk indicates a statistically significant difference ($P < 0.05$).

concentrated at a cluster of pleomorphic tubules and vesicles in the pericentrosomal region of the cell (Movie S1 and *SI Appendix*, Fig. S1). In fixed cells, mCherry-CvpA–containing vesicles near the plasma membrane labeled with antibodies against clathrin and early endosome antigen 1 (EEA1), whereas mCherry-CvpA vesicles near the pericentrosomal region labeled with antibodies against LAMP1 (Fig. 3*A*). In contrast, antibodies against the ER proteins p61 and ERGIC53 (*SI Appendix*, Fig. S2*A*) and the Golgi protein giantin (*SI Appendix*, Fig. S3*A*) did not label structures containing mCherry-CvpA. Finally, when expressed in *C. burnetii*-infected HeLa cells, mCherry-CvpA localized to the LAMP1-positive PV membrane (Fig. 3*A*). Collectively, these data suggest that CvpA traffics through endolysosomal, but not secretory, compartments that interact with the PV.

To characterize the endosomal compartment in which CvpA traffics, HeLa cells coexpressing mCherry-CvpA and GFP-tagged Rab GTPases were examined by live-cell microscopy. MCherry-CvpA partially localized with Rab5-GFP in the periphery and center of the cell (Fig. 3*B*). Prominent pericentrosomal localization was observed with Rab11-GFP, and partial colocalization was observed with Rab7 (Fig. 3*B*). Consistent with the lack of colocalization with ER or Golgi proteins, mCherry-CvpA did not

Table 1. Colocalization of HeLa cell proteins with mCherry-CvpA

Protein	Structure labeled	CvpA localization
Endocytic system		
Clathrin	CCV	+
EEA1	EE	+
LAMP1	Endosomes, PV	+
TfR	EE, RE	+
Secretory system		
p61	ER	–
ERGIC53	ERGIC	–
Giantin	Golgi	–
GFP-tagged Rab GTPases		
Rab5	CCV, EE	±
Rab6A	Golgi	–
Rab7	LE	±
Rab9	Golgi	–
Rab11	RE	+

Scoring of mCherry-CvpA localization is indicated with the following markers: (+) strong colocalization, (±) partial colocalization, (–) no colocalization. CCV, clathrin-coated vesicle; EE, early endosome; EEA1, early endosome antigen 1; ER, endoplasmic reticulum; ERGIC, ER-Golgi intermediate compartment; LAMP1, lysosomal-associated membrane protein 1; LE, late endosome; RE, recycling endosome; TfR, transferrin receptor.

colocalize with the secretory system Rab GTPases Rab6A and Rab9 (*SI Appendix*, Fig. S2*B*). Prominent colocalization with Rab5 and Rab11 suggested that mCherry-CvpA traffics to peripheral sorting endosomes (SEs) and pericentrosomal recycling endosomes (REs), where endocytic cargo is sorted and delivered to other vesicular compartments or recycled back to the cell surface (37, 38).

The pericentrosomal region of a HeLa cell contains pleomorphic vesicles derived from both endosomal (e.g., REs) and secretory compartments (e.g., Golgi). To confirm that CvpA trafficked endosomally, cells expressing mCherry-CvpA were treated with brefeldin A (BFA) that disrupts vesicle coats, leading to tubulation of endosomal compartments and fragmentation of Golgi stacks (39). BFA dispersed the Golgi, but not pericentrosomal mCherry-CvpA (*SI Appendix*, Fig. S3*A*). Moreover, in peripheral regions of BFA-treated cells, mCherry-CvpA localized to tubules that stained with antibodies against transferrin (Tf) receptor (TfR). This result is consistent with mCherry-CvpA trafficking within REs (38, 40). To ascertain whether CvpA expression alters endocytosis of Tf, we measured uptake of fluorescent Tf (Tf488) in HeLa cells ectopically expressing mCherry-CvpA. Compared with untreated cells or cells expressing mCherry alone, a significant 23% reduction ($P < 0.05$) in Tf uptake was observed in cells expressing mCherry-CvpA (*SI Appendix*, Fig. S3*B*), suggesting that CvpA expression perturbs Tf trafficking mechanisms.

To assess whether the distribution of clathrin is altered in response to secretion of native CvpA, we quantified by confocal immunofluorescence microscopy the density of PV-associated and cytoplasmic clathrin in Vero cells infected with wild-type *C. burnetii*, the *cvpA* mutant, or the complemented *cvpA* mutant. Micrographs showed a higher density of clathrin adjacent to PV formed by wild-type *C. burnetii* and the complemented *cvpA* mutant relative to the *cvpA* mutant (*SI Appendix*, Fig. S4*A*). When the clathrin signal was quantified, the ratio of PV-associated to cytoplasmic clathrin was significantly higher ($P < 0.05$) in cells infected with wild-type *C. burnetii* or the complemented *cvpA* mutant compared with cells infected with the *cvpA* mutant (*SI Appendix*, Fig. S4*B*). These data are consistent with a positive role for CvpA in co-opting clathrin for PV formation.

AP2 Binds CvpA Endocytic-Sorting Motifs. Adaptor proteins recognize endocytic sorting motifs like those found within CvpA and coordinate sorting and recycling within the endosomal system (31, 38), raising the possibility that similar mechanisms control CvpA trafficking. To evaluate their importance for CvpA endosomal trafficking, the three dileucine and two tyrosine-sorting motifs (Fig. 1) were mutated by making LL-to-AA and Y-to-A

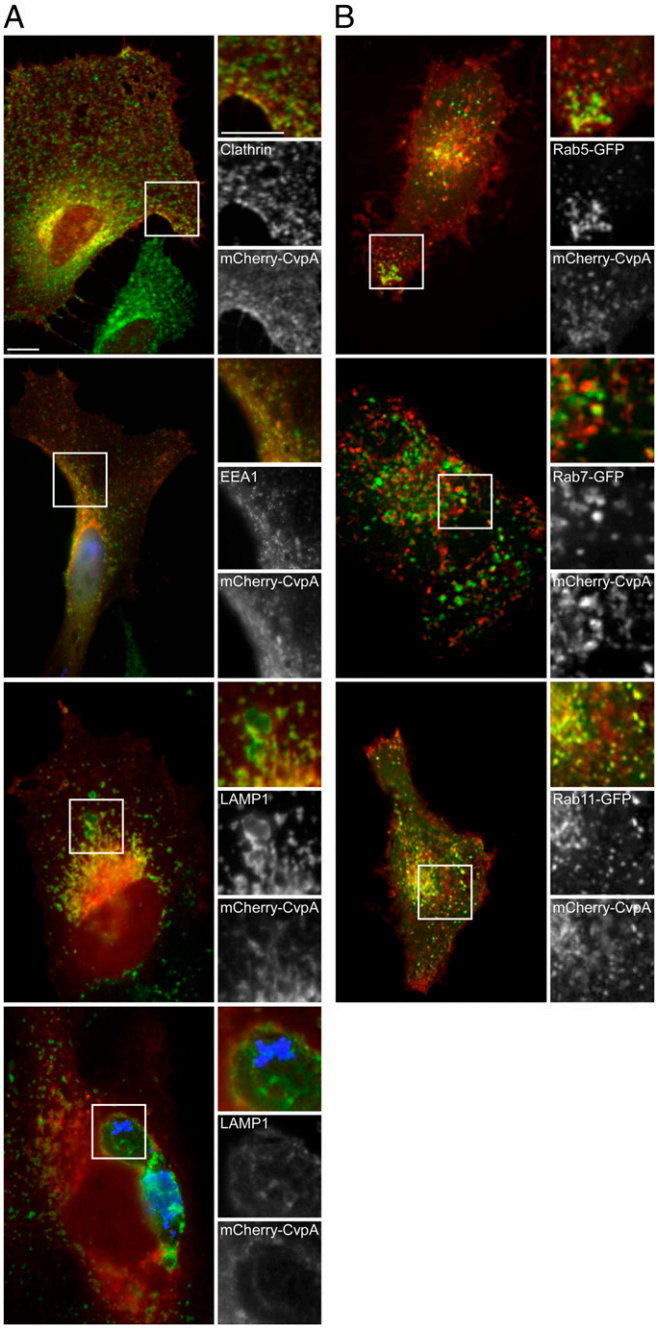

Fig. 3. Ectopically expressed mCherry-CvpA localizes to endocytic vesicles and traffics to pericentrosomal REs. (*A*) Representative micrographs of fixed HeLa cells expressing mCherry-CvpA (red) and immunostained for the vesicle proteins clathrin, EEA1, and LAMP1 (green). (*Bottom*) A cell infected with *C. burnetii* where bacteria and LAMP1 are immunostained blue and green, respectively. (*B*) Micrographs of live cells coexpressing mCherry-CvpA (red) and the GFP-tagged Rab GTPases Rab5, Rab7, or Rab11 (green). (Scale bar, 10 μm.)

amino acid substitutions, respectively. A Tyr1/Tyr2 double mutant was also constructed. The cellular localization of ectopically expressed mutant proteins fused to mCherry was then examined by fluorescence microscopy and scored according to three phenotypes: tubulovesicular, punctate, or diffuse (Fig. 4). In contrast to the 100% tubulovescular localization of wild-type mCherry-CvpA, more than 90% of cells expressing mCherry-CvpA with mutated DiLeu2, DiLeu3, Tyr1, or Tyr1/Tyr2 motifs exhibited diffuse localization. The DiLeu1 mutation resulted in a punctate and diffuse appearance in 81% and 19% of the cells, respectively, whereas the Tyr2 mutation resulted in tubulovesicular localization resembling wild-type mCherry-CvpA in 95% of cells and puncta in the remaining 5% of cells. The latter result implies that mutation of Tyr2 produces minor trafficking defects without disrupting membrane association. Collectively, these data suggest that DiLeu1, DiLeu2, DiLeu3, and Tyr1 mediate CvpA membrane association via interactions with AP complexes.

Pull-down assays were then performed to evaluate interactions of CvpA sorting motifs with the AP complexes (41). CvpA 30mer peptides containing DiLeu1 (aa 2–31), Tyr1–2 (aa 52–81),

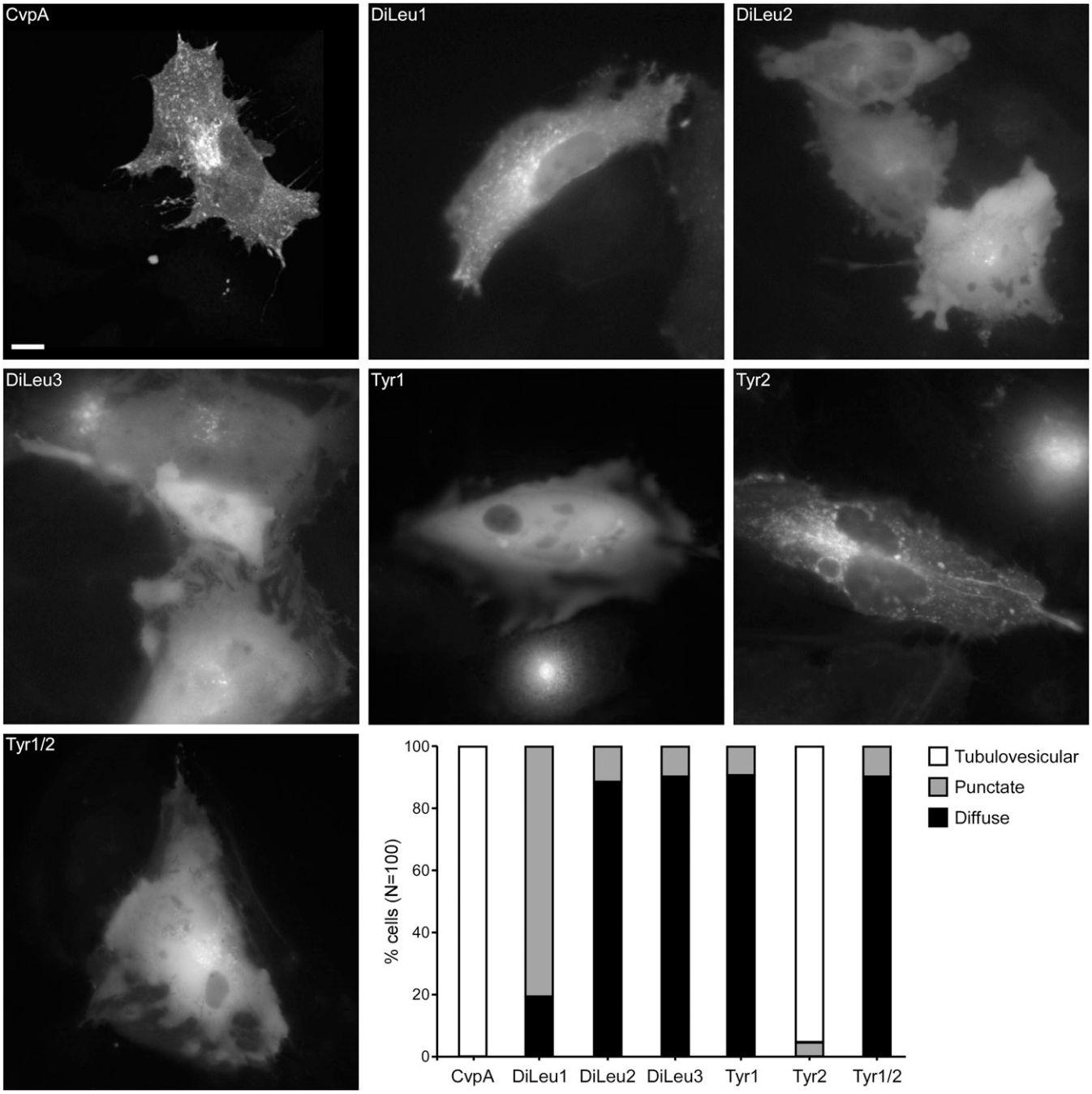

Fig. 4. Mutation of CvpA endocytic sorting motifs disrupts vesicular localization of mCherry-CvpA. Representative micrographs of HeLa cells expressing mCherry-CvpA or mCherry-CvpA proteins where diluecine residues were substituted with dialanine in DiLeu1, Dileu2, and Dileu3, and tyrosine residues were substituted with alanine in Tyr1, Tyr2, and Tyr1/Tyr2. (Scale bar, 10 μm.) (*Lower Right*) Graph showing the percentage of HeLa cells exhibiting tubulovesicular, punctate, or diffuse localization of ectopically expressed mCherry-CvpA proteins (n = 100).

DiLeu2 (aa 172–201), or DiLeu3 (aa 299–328) (Fig. 1) endocytic sorting motifs and bearing an N-terminal glutathione S-transferase (GST) tag were incubated overnight with HeLa cell lysates (41). GST peptides were collected with glutathione agarose beads, and interactions with clathrin heavy chain (CLTC), AP1, AP2, or AP3 were assessed by immunoblotting (Fig. 5*A*). AP1, AP2, and AP3 heterotetrameric complexes are composed of the four subunits γ/β/μ/σ-1, α/β/μ/σ-2, and δ/β/μ/σ-3, respectively (29, 30). AP2 subunits α and β interacted with all four GST-30mer peptides whereas clathrin bound only GST-Tyr1–2 (Fig. 5*A*). Given that CvpA lacks known clathrin-binding motifs, and that clathrin binds an LLNLD motif in the β-subunit of AP complexes (42), an indirect interaction mediated by the β-subunit of AP2 likely links the peptide Tyr1–2 to clathrin. AP1 (γ-subunit) or AP3 (δ-subunit) did not interact with any CvpA peptide. Alanine substitution of dileucine or tyrosine within the sorting motifs abolished binding by AP2 and clathrin (Fig. 5*B*). Full-length GST-CvpA expressed in *E. coli* was insoluble, precluding purification of native protein. Therefore, AP2 binding to full-length CvpA was assessed by ectopically expressing CvpA containing an N-terminal biotinylation sequence in HeLa cells, followed by pull-down with streptavidin beads. Endogenous AP2 (β-subunit) and clathrin bound to biotinylated CvpA, but not to control biotinylated mCherry (Fig. 5*C*).

To examine the importance of CvpA sorting motifs in the context of secreted native protein, we assessed growth in THP-1 macrophages of *C. burnetii* Δ*cvpA* expressing a mutant version of *cvpA* encoding a protein where diluecine residues were changed to dialanine in DiLeu1, Dileu2, and Dileu3 and tyrosine residues were changed to alanine in Tyr1 and Try2. Growth of *C. burnetii* Δ*cvpA*-expressing mutant CvpA was significantly reduced compared with organisms expressing wild-type CvpA ($P < 0.05$) (*SI Appendix*, Fig. S5). Expression of mutant CvpA did modestly improve growth over the noncomplemented strain, which we attribute to the mutant protein's ability to still interact with beneficial factors, perhaps via its leucine-rich repeat. Collectively, these data, and the intracellular trafficking behavior of mCherry-CvpA, support the conclusion that CvpA dileucine and tyrosine motifs bind AP2-clathrin–coated vesicles. Indeed, of the clathrin adaptor complexes, AP2 is specifically associated with endocytosis of cargo molecules at the plasma membrane and transport to early endosomal compartments (29, 30, 43).

AP2 and Clathrin Are Required for Intracellular Growth of *C. burnetii*. CvpA interactions with AP2 and clathrin suggested that AP2-clathrin–mediated vesicular transport is important for intracellular growth of *C. burnetii*. To investigate this possibility, AP2 and clathrin activities were inhibited by depleting cellular protein levels with siRNA. To ensure inhibition of AP2 adaptor function, depletion of both β- and μ-subunits was conducted (41). Cells were infected with *C. burnetii* at 2 d post siRNA treatment (day 0 post infection), a time point where significant reductions in AP2 subunits and clathrin were detected by immunoblotting (Fig. 6*A*). At day 0 post infection, there was no difference in recoverable GE between cells treated with nontargeting siRNA and cells depleted of the targeted proteins, indicating that clathrin-mediated processes are not involved in *C. burnetii* uptake (*SI Appendix*, Table S1). At 1 and 3 d post infection, *C. burnetii* replication was the same, based on fold increase in GE, in cells treated with nontargeting or targeting siRNA (Fig. 6*B* and *SI Appendix*, Table S1). However, at 5 d post infection, cells depleted of clathrin, or AP2 subunits β and μ, showed 81% and 72% reductions in replication, respectively, relative to cells treated with nontargeting siRNA (Fig. 6*B* and *SI Appendix*, Table S1). Reduced *C. burnetii* replication correlated with a significant decrease in PV size (*SI Appendix*, Fig. S6 *A* and *B*). Growth

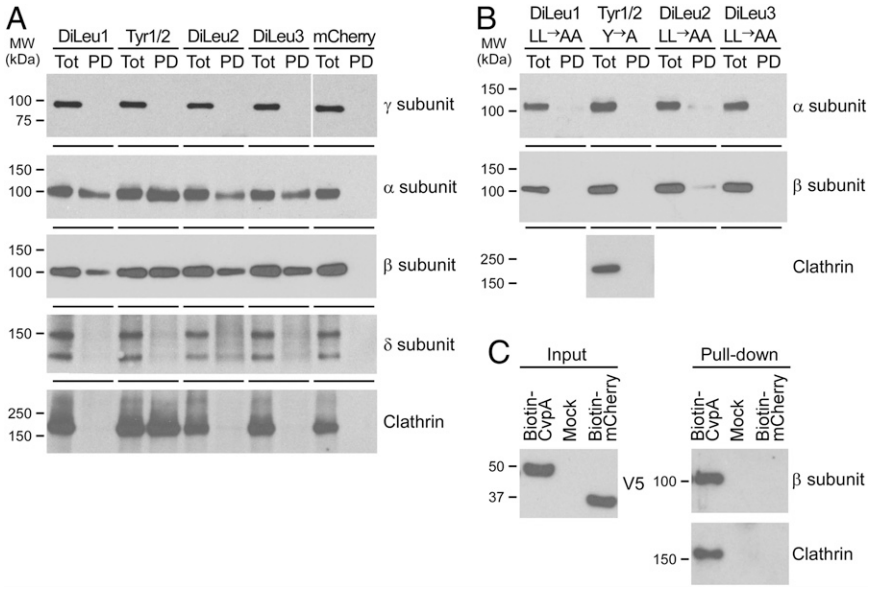

Fig. 5. CvpA endocytic sorting motifs interact with AP2 and clathrin. (*A*) Pull-down assays using HeLa cell lysates and GST fusions to 30mer peptides containing the CvpA endocytic sorting motifs DiLeu1 (aa 2–31), DiLeu2 (aa 172–201), DiLeu3 (aa 299–328), or Tyr1/Tyr2 (aa 52–81). GST peptides and interacting proteins were collected with glutathione agarose beads and analyzed by immunoblot with antibodies against clathrin and clathrin adaptor complex subunits present in AP1 (subunit γ), AP2 (subunits α and β), or AP3 (subunit δ). Pull-down with GST-mCherry was used as a negative control. (*B*) Pull-down assays using GST fusions to 30mer peptides containing endocytic sorting motifs where diluecine residues were substituted with dialanines, and tyrosine residues were substituted with alanine. Immunoblotting was conducted with antibodies against the α- and β-subunits of AP2 or clathrin (Tyr1/Tyr2 pull-down). (*C*) Pull-down assay using biotinylated full-length CvpA. CvpA containing an N-terminal biotinylation signal and a C-terminal V5 tag was expressed in HeLa cells and then collected from cell lysates using streptavidin beads. Cells expressing biotin-mCherry or nontransfected cells (Mock) were used as negative controls. Immunoblot detection of the V5 tag was used to assess equal expression of biotin-tagged proteins (*Left*). Pull-down samples were immunoblotted with antibodies recognizing clathrin and the β-subunit of AP2 and clathrin (*Right*).

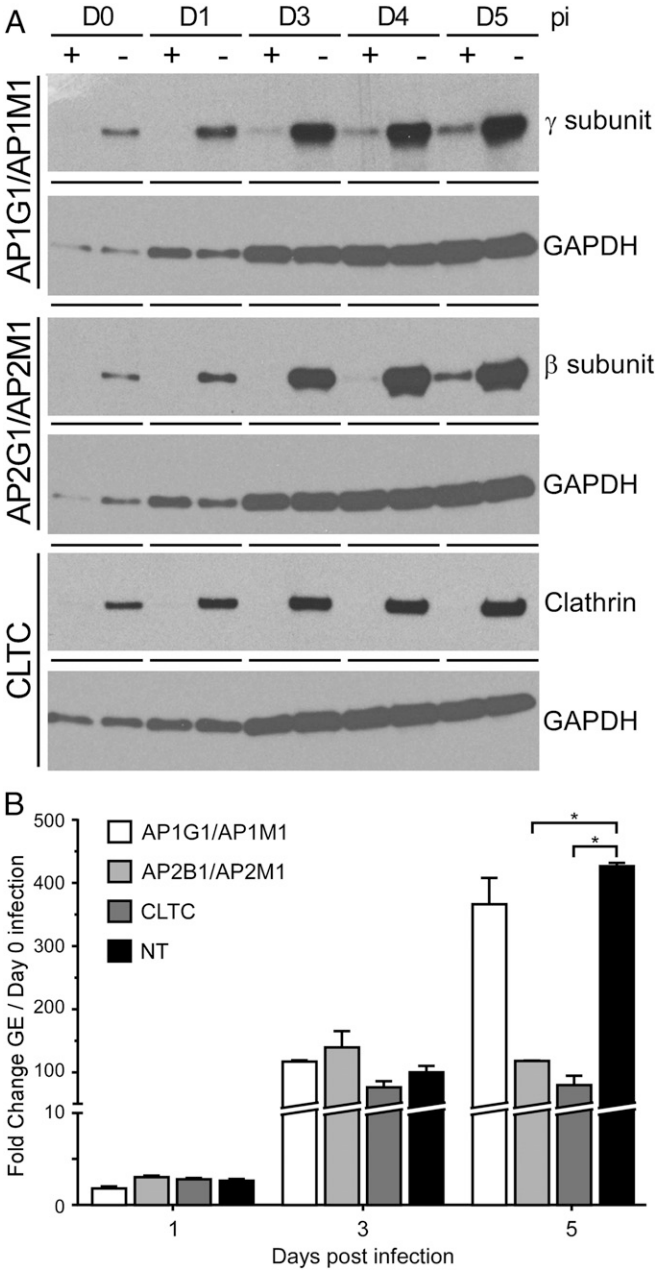

Fig. 6. Depletion of cellular AP2 or clathrin inhibits *C. burnetii* intracellular growth. (*A*) Protein expression in cells treated with targeting (+) or nontargeting (NT) (–) siRNA at 0, 1, 3, 4, or 5 d post infection (pi). HeLa cells were transfected with siRNA to deplete γ- and μ-subunits of the AP1 complex (AP1G1 and AP1M1 siRNA), β- and μ-subunits of AP2 (AP2B1 and AP2M1 siRNA), or clathrin (CLTC siRNA) and then infected with *C. burnetii* 2 d later (day 0 pi). Cell lysates were immunoblotted with antibodies against the AP1 γ-subunit, AP2 β-subunit, or clathrin to assess protein depletion and with antibody against GAPDH to confirm equal protein loading. (*B*) *C. burnetii* replication in HeLa cells depleted of AP1 subunits, AP2 subunits, or clathrin by siRNA. *C. burnetii* GEs at 1, 3, and 5 d pi were compared with GEs at day 0 pi to determine fold increases. Results are expressed as the means of two biological replicates and are representative of two independent experiments. Error bars indicate SE from the means, and an asterisk indicates a statistically significant difference ($P < 0.05$).

inhibition was specific to AP2-dependent transport as depletion of the γ- and μ-subunits of AP1 did not inhibit *C. burnetii* replication nor reduce PV size (Fig. 6*B* and *SI Appendix*, Fig. S6 *A* and *B*). These data demonstrate that clathrin-dependent transport is critical for *C. burnetii* growth and PV biogenesis. Collectively, our results suggest that, once secreted via the T4BSS, CvpA binds to AP2-clathrin complexes and subverts associated vesicular transport mechanisms that promote *C. burnetii* intracellular replication.

Discussion

Expected among the repertoire of identified *C. burnetii* Dot/Icm T4BSS substrates are effectors that benefit pathogen replication by modulating host vesicular trafficking. Here, we describe CvpA, a T4BSS effector that engages clathrin transport machinery. Making use of methods for targeted gene deletion (15), we generated a *C. burnetii* Δ*cvpA* mutant that exhibits severe intracellular growth defects rescuable by gene complementation. CvpA traffics dynamically within recycling compartments of the endosomal system by a mechanism requiring dileucine- and tyrosine-based sorting motifs that specifically interact with the clathrin adaptor complex AP2. Inhibition of AP2 or clathrin with siRNA markedly reduces bacterial replication and PV size, verifying that AP2-clathrin vesicle transport mechanisms targeted by CvpA support intracellular growth of *C. burnetii*. Engagement of the AP2-clathrin pathway by CvpA is an effector activity that benefits biogenesis of a pathogen-occupied vacuole.

Selection and packaging of cargo molecules for endocytosis into clathrin-coated transport vesicles is a complex process involving adaptor protein recognition of sorting motifs in the cytoplasmic domains of transmembrane proteins (29, 32, 38, 44). Clathrin adaptor proteins bind endocytic sorting motifs, and with the help of recruited accessory proteins, link cargo proteins to budding CCVs for transport to vesicular compartments of the cell (38, 45, 46). The heterotetrameric clathrin adaptor complexes AP1, AP2, and AP3 bind both dileucine and tyrosine sorting motifs like those found in CvpA (29), which raises the possibility that CvpA targets clathrin-mediated endocytosis. Mutations within either dileucine- or tyrosine-sorting motifs disrupt tubulovesicular localization of ectopically expressed CvpA, indicating that both types of sorting motifs are important for CvpA membrane association. Moreover, CvpA peptides containing sorting motifs and full-length protein specifically interact with AP2 subunits, suggesting that CvpA membrane interactions result from binding of membrane-bound AP2.

AP1, AP2, and AP3 heterotetramers are composed of two large subunits (γ/β1, α/β2, δ/β3), a medium subunit (μ), and a small subunit (σ) (29, 30). Each AP complex recognizes a subset of sorting motifs, and the variant amino acids within [DERQ]XXXL[LI] and YXXΦ sequences define the specificity of signal recognition (47–49). Disruption of AP complex interactions with sorting motifs can lead to missorting of cargo proteins back to the plasma membrane (50–53). The AP2 complex recognizes proteins with more divergent dileucine motifs and binds tyrosine motifs with higher affinity than AP1 and AP3, a property thought to promote retrieval of proteins missorted to the plasma membrane (54, 55). GST fusions to peptides containing the CvpA dileucine- or tyrosine sorting motifs interacted with α- and β-subunits of AP2. The Tyr1/Tyr2 peptide appeared to bind more α- and β-subunits than the other peptides and also interacted with clathrin. The β-subunit of AP2 contains a LLDLD motif bound by clathrin, thereby linking the complex to clathrin coats (42). Moreover, the β-subunit of AP2 is sufficient to drive clathrin coat assembly (56). Thus, the enhanced binding of the β-subunit of AP2 to CvpA tyrosine sorting motifs may explain the pull-down of clathrin.

Knockdown of clathrin or AP2 subunits with siRNA was conducted to better understand their roles in *C. burnetii* growth (41, 53, 57). Growth of *C. burnetii* at 1 and 3 d post infection is similar in cells depleted of AP2 or clathrin relative to cells treated with nontargeting or AP1 siRNAs. However, at 5 d post infection, a time point when *C. burnetii* is replicating exponentially and pronounced PV expansion is occurring (6, 7), no additional

growth was observed in cells depleted of AP2 subunits β and μ or clathrin relative to control cells. Janvier et al. (58) reported siRNA ablation of AP2, but not AP1 or AP3, inhibits delivery of LAMPs to lysosomes. Inhibition of *C. burnetii* growth in response to AP2 and clathrin knockdown was equivalent, indicating that AP2 likely regulates a significant portion of clathrin transport events required for robust pathogen replication and PV enlargement.

Coat complexes, such as clathrin, coat protein I (COPI), and COPII, are recruited to the cytosolic surface of donor vesicles, allowing selective transfer of proteins to acceptor compartments (30, 45). AP2-clathrin coats regulate budding of vesicles from the plasma membrane into the cell cytoplasm where CCVs uncoat to form primary vesicles that fuse with peripheral early endosomes (EEs) (38). The majority of lipids and proteins acquired through endocytosis returns to the cell surface, whereas a fraction is delivered to late endosome (LEs) or the TGN. Sorting and recycling of endocytic cargo is predominantly associated with EEs, which can be subdivided into peripheral SEs and pericentrosomal REs (37, 38). CvpA localized to peripheral vesicles containing EEA1 and Rab5, known regulators of SE fusion and recycling back to the cell surface, respectively (38). Maturation of SEs is accompanied by decreased fusion with primary endocytic vesicles, and the formation of tubular transport intermediates that translocate toward the center of the cell and fuse with longer-lived Rab11-positive REs, the major sorting compartment of the endosomal system (37, 38). CvpA localized to pericentrosomal LAMP1-positive tubules and vesicles harboring Rab11 and TfR. Proper trafficking of numerous receptors, such as TfR, β2-adrenergic receptors, and epidermal growth factor receptor, through REs is dependent upon Rab11 activity (40, 59, 60). CvpA localized to TfR-positive tubular endosomes following BFA treatment (39), further establishing CvpA's residence within the endosomal recycling compartment. Disruption of Rab11 or AP2 blocks endocytosis of Tf and TfR trafficking (40, 43, 60, 61), which might explain the reduced uptake of Tf in cells ectopically expressing CvpA. Reduced Tf internalization could also result from CvpA-dependent recruitment of clathrin, thereby making less clathrin available for transferrin endocytosis. The observation that ectopically expressed CvpA localizes to the PV membrane, and that native expression of CvpA by *C. burnetii* is associated with clathrin recruitment to the PV, further supports the notion that CvpA traffics within endosomal compartments that supply material for *C. burnetii* vacuole biogenesis.

C. burnetii must sequester substantial amounts of lipid and protein from host endomembrane compartments to form its large phagolysosome-like vacuole. This process likely involves subversion of vesicular trafficking pathways by multiple *C. burnetii* T4BSS effectors. Our current findings support a model wherein *C. burnetii* CvpA co-opts clathrin transport mechanisms to acquire endolysosomal membrane components for PV biogenesis and intracellular growth. Precedence for pathogen subversion of adaptor function has been established for the HIV-1 proteins, Nef and Gag. Nef endocytic sorting motifs are recognized by AP2 and induce internalization of major histocompatibility complex receptors and avoidance of host defenses (50, 62–64). Gag–AP3 interactions recruit the ESCRT protein TSG101 to promote viral particle assembly (41, 65). In addition to endocytic sorting motifs, other CvpA domains, such as the LRR domain, likely confer additional activities that benefit *C. burnetii* replication.

Materials and Methods

Cell Culture. *C. burnetii* Nine Mile phase II (clone 4, RSA439) was cultured axenically in ACCM-2 as previously described (12, 16). *E. coli* TOP10 and BL21-AI (Invitrogen) were grown in Luria–Bertani medium for recombinant DNA procedures and protein purification. THP-1 [TIB-202; American Type Culture Collection (ATCC)] human monocytic cells, Vero (CCL-81; ATCC) African green monkey kidney cells, and HeLa (CCL-2; ATCC) human cervical epithelial cells were cultured according to ATCC guidelines.

***C. burnetii* Plasmids and Cloning.** The *C. burnetii* Δ*cvpA* mutant and complement strains were generated by previously described methods (15, 16). Briefly, targeted deletion of Δ*cvpA* and insertion of a Kan cassette was accomplished via homologous recombination with a pJC-CAT suicide plasmid. Clonality of *C. burnetii* Δ*cvpA* was confirmed by PCR, and the strain was complemented with *cvpA* under control of its native promoter using pMiniTn7T-CAT. A modified *cvpA* gene was synthesized (Genscript) for expression of CvpA-containing dileucine to dialanine substitutions in the three dileucine motifs and tyrosine-to-alanine substitutions in the two Tyr motifs and inserted into pMiniTn7T-CAT for generation of the *C. burnetii* Δ*cvpA* strain expressing mutant CvpA. For adenylate cyclase assays, *cvpA* was amplified using gene-specific primers and cloned into the SalI site of linearized pJB-CAT-CyaA using In-Fusion (Promega) (23). Primer sequences and plasmids for generation of protein expression constructs are detailed in *SI Appendix*, Tables S2 and S3. In general, PCR products were cloned into the pENTR/D (Invitrogen) entry vector and moved to Gateway compatible destination vectors. MCherry-CvpA was expressed in HeLa cells from an anhydrotetracycline (aTc)-inducible promoter using pT-REx-DEST30 (Invitrogen) modified for expression of mCherry N-terminal fusion proteins. The Rab GTPase expression plasmids pEGFP-Rab5, Rab6A, Rab7, Rab9, and Rab11 were a generous gift from M. A. Scidmore, Cornell University (Ithaca, NY). GST-tagged peptides were expressed in *E. coli* using pDEST15 (Invitrogen). Genes conferring resistance to chloramphenicol, kanamycin, or ampicillin are approved for *C. burnetii* transformation studies by the Rocky Mountain Laboratories Institutional Biosafety Committee and the Centers for Disease Control and Prevention, Division of Select Agents and Toxins Program (Atlanta).

Bioinformatics. *C. burnetii* genes with consensus PmrA regulatory elements have been previously described (36). Endocytic sorting motifs within CvpA were identified using ELM, the database of eukaryotic linear motifs (31), and the LRR was identified using the Pfam database of the protein families tool (66) and the protein Basic Local Alignment Search Tool.

CyaA Translocation Assay. THP-1 cells (1×10^5 per well) in 24-well plates were differentiated into macrophage-like cells by incubation overnight in RPMI (Invitrogen) medium containing 10% (vol/vol) FBS and 200 nM phorbol myristate acetate (PMA) (Sigma-Aldrich). Cells were washed once with RPMI plus 10% FBS, infected with 1×10^6 *C. burnetii* harboring pJB-CAT-CyaA-CvpA or vector alone, and incubated in RPMI plus 10% FBS for 48 h. The concentration of cAMP in lysates from infected cells was determined using the cAMP enzyme immunoassay (GE Healthcare) as previously described (16).

***C. burnetii* Growth Assays.** PMA-differentiated THP-1 cells (1×10^5 per well) in a 24-well plate were infected with *C. burnetii* at a multiplicity of infection (MOI) of 0.5 by centrifugation of plates at $500 \times g$ for 20 min. Cells were washed once with RPMI plus 10% (vol/vol) FBS and replenished with the same medium. This time point was considered 0 h post infection. At the indicated time points, cells were harvested by trypsinization and pelleted by centrifugation at $15{,}000 \times g$ for 5 min. Cell pellets were resuspended in H_2O, bead-beaten, and boiled, and *C. burnetii* genomic equivalents were determined by quantitative PCR as described previously (16).

Ectopic Expression and Fluorescence Microscopy. HeLa cells (2×10^4 per well) in a 24-well plate were cultured in DMEM (Invitrogen) containing 10% FBS for 6 h. Using FuGENE 6 (Promega), cells were then transfected with 500 μg of pT-REx-DEST30/*N*-mCherry-CvpA fusion protein constructs and 250 μg of the plasmid pcDNA 6/TR (Invitrogen) for constitutive expression of the tet-repressor protein. For coexpression of mCherry-CvpA and GFP-tagged Rab GTPases, HeLa cells were cotransfected with 500 μg of pT-REx-DEST30/*N*-mCherry-CvpA, 250 μg pcDNA 6/TR, and 250 μg of the respective EGFP-Rab plasmids. The following day, cells were replenished with fresh growth medium containing 1 μg/mL aTc (Sigma) and incubated 24 h to induce protein expression. Confocal live-cell imaging was conducted using a modified Perkin-Elmer UltraView spinning-disk confocal system connected to a Nikon Eclipse Ti-E inverted microscope. For immunofluorescence, cells were fixed with 2.5%(vol/vol) paraformaldehyde and permeablilzed with PBS containing 0.05% saponin and 5% (vol/vol) FBS. Following staining with primary and secondary antibodies, coverslips were mounted using Prolong Gold with DAPI (Invitrogen) and imaged with a Nikon Eclipse TE-2000 inverted microscope equipped with a Cool Snap digital camera. Uptake of transferrin Alexa Fluor 488 (Tf488) (Invitrogen) in cells expressing mCherry-CvpA was

measured as previously described (67). Twenty-five cells were measured per condition for each experiment (n = 2) with identical threshold settings. ImageJ software (W. S. Rasband, National Institutes of Health, Bethesda) was used to quantify Tf488 intensity per cell area (67). The density of PV-associated and cytoplasmic clathrin in Vero cells infected with *C. burnetii* strains was measured using confocal immunofluorescence microscopy. Vero cells were infected for 5 d, then fixed, and stained for LAMP-1 and clathrin as described above. Confocal images (0.39-μm sections) were collected using a LSM710 confocal laser-scanning microscope (Carl Zeiss Micro Imaging). The intensity of the clathrin signal at 0–20 pixels (2.6 μm) directly adjacent to the PV membrane was compared with the signal in the cytoplasmic region 20–40 pixels away from the PV membrane. PV-adjacent and cytoplasmic regions were demarked by 20-pixel-diameter circles (3×), and ImageJ was used to measure the clathrin signal intensities within each circle. Ten cells infected with individual *C. burnetii* strains were measured per experiment (n = 3). The PV-associated signal was divided by the cytoplasmic signal to yield the plotted clathrin intensity values.

Pull-Down Assays. The CvpA endocytic sorting motifs DiLeu1, Tyr1–2, DiLeu2, and DiLeu3 contained in 30mer peptides were fused to GST to assess motif interactions with AP complexes using established pull-down assay methods (41, 68) (*SI Appendix*). Peptides with N-terminal GST tags were purified from *E. coli* BL21-AI by affinity chromatography with glutathione agarose beads (Pierce), dialyzed against pull-down buffer [25 mM Hepes–KOH (pH 7.2), 125 mM potassium acetate, 2.5 mM magnesium acetate, 0.4% Triton X-100, and protein inhibitor mixture (P8340, Sigma)], and concentrated using an Amicon Ultra Ultracel-10 centrifugal filter unit (Millipore). In a total volume of 1 mL of pull-down buffer, 1 mg of GST-peptide was mixed with 1 mg of HeLa cell lysate and incubated overnight at 4 °C in a 1.5-mL siliconized microcentrifuge tube. Aliquots from pull-down mixtures were collected for total protein samples. Fifty microliters of packed glutathione agarose beads were added to pull-down mixtures that were incubated for 2 h at 4 °C and then collected by centrifugation at 750 × g for 1 min. Beads were washed extensively with wash buffer (pull-down buffer containing 0.1% Triton X-100). Bead pellets were resuspended in 50 μL SDS/PAGE sample buffer and boiled to release bound proteins. For immunoblotting, 10 μL of sample aliquots was separated by SDS/PAGE, transferred to polyvinylidene difluoride membranes (Millipore), and probed with the indicated antibodies. SDS/PAGE gels were also stained with Coomassie Brilliant Blue (BioRad) to confirm equal loading.

For pull-downs with full-length CvpA, pcDNA 6.2/*N*-mCherry DEST (22) was modified for expression of proteins with a N-terminal biotin tag and C-terminal V5 tag (*SI Appendix*). HeLa cells (3×10^5 per well) in a six-well plate were transfected as described above. Cells were incubated for 48 h in DMEM plus 10% (vol/vol) FBS and 200 μM biotin and then lysed in 1 mL of lysis buffer [50 mM Tris·HCl (pH7.5), 100 mM NaCl, 2 mM MgCl, 1% Triton ×100, 10% (vol/vol) glycerol, and protease inhibitor mixture]. Insoluble material was pelleted (15,000 × g at 4 °C for 30 min), and biotin-CvpA complexes were collected with streptavidin Dynabeads (Invitrogen) according to supplier instructions. Samples were immunoblotted as above.

siRNA Knockdown. ON-TARGETplus SMARTpool siRNA duplexes against AP1 subunits γ and μ (AP1G1, AP1M1), AP2 subunits β and μ (AP2B1 AP2M1), and CLTC, as well as nontargeting siRNA, were obtained from Dharmacon. DharmaFECT1 (Dharmacon) was used to transfect HeLa cells (2×10^4 cells per well) in a 24-well plate with siRNA duplexes according to instructions. At the indicated time points, cells were lysed with 200 μL SDS/PAGE sample buffer per well, transferred to a microcentrifuge tube, and boiled for 5 min. To compare protein depletion in cells treated with targeting and nontargeting siRNAs, 10 μL of each lysate was immunoblotted with antibodies against AP1 γ-subunit, AP2 β-subunit, or clathrin. To demonstrate equal protein loading, the immunoblots were stripped and reprobed with antibody against GAPDH. Efficient knockdown of protein by targeting siRNAs was confirmed at 2 d post transfection, at which point cells were infected with *C. burnetii* at an MOI of 1 as above. At the indicated times post infection, cells were processed for immunoblotting, quantitative PCR, and immunofluorescence as described above.

Antibodies. EEA-1 (2411S), GAPDH (2118S) (Cell Signaling), LAMP1 (ab24170), LAMP1 (ab25630), clathrin (ab21679) (Abcam), β-adaptin (610382), γ-adaptin (51-9001897), δ-adaptin (611328), p61 (612584), p230 (611280) (BD Biosciences) transferrin receptor (136800) (Life Technologies), V5-tag (46-0705), Alexa Fluor 488 goat anti-mouse (A11029), Alexa Fluor 488 goat anti-rabbit (A11034) (Invitrogen), Giantin (PRB-114C) (Covance), ERGIC53 (G1/93) (Alexis Biochemicals), and guinea pig anti-*C. burnetii* serum (16).

Statistical Analysis. Statistical analyses were conducted using Prism software (GraphPad Software, Inc.) to perform unpaired Student t test or one-way ANOVA using Tukey's post test. P values less than 0.05 were considered significant.

ACKNOWLEDGMENTS. We thank Daniel E. Voth for technical contributions, Olivia Steele-Mortimer for helpful suggestions, Austin Athman for graphics support, and Jean Celli for critical review of this manuscript. This work was supported by the Intramural Research Program of the National Institutes of Health, National Institute of Allergy and Infectious Disease.

1. Maurin M, Raoult D (1999) Q fever. *Clin Microbiol Rev* 12(4):518–553.
2. Voth DE, Heinzen RA (2007) Lounging in a lysosome: The intracellular lifestyle of *Coxiella burnetii*. *Cell Microbiol* 9(4):829–840.
3. Alix E, Mukherjee S, Roy CR (2011) Subversion of membrane transport pathways by vacuolar pathogens. *J Cell Biol* 195(6):943–952.
4. Isberg RR, O'Connor TJ, Heidtman M (2009) The *Legionella pneumophila* replication vacuole: Making a cosy niche inside host cells. *Nat Rev Microbiol* 7(1):13–24.
5. Campoy EM, Zoppino FC, Colombo MI (2011) The early secretory pathway contributes to the growth of the *Coxiella*-replicative niche. *Infect Immun* 79(1):402–413.
6. Coleman SA, Fischer ER, Howe D, Mead DJ, Heinzen RA (2004) Temporal analysis of *Coxiella burnetii* morphological differentiation. *J Bacteriol* 186(21):7344–7352.
7. Howe D, Melnicáková J, Barák I, Heinzen RA (2003) Maturation of the *Coxiella burnetii* parasitophorous vacuole requires bacterial protein synthesis but not replication. *Cell Microbiol* 5(7):469–480.
8. Romano PS, Gutierrez MG, Berón W, Rabinovitch M, Colombo MI (2007) The autophagic pathway is actively modulated by phase II *Coxiella burnetii* to efficiently replicate in the host cell. *Cell Microbiol* 9(4):891–909.
9. Akporiaye ET, Rowatt JD, Aragon AA, Baca OG (1983) Lysosomal response of a murine macrophage-like cell line persistently infected with *Coxiella burnetii*. *Infect Immun* 40(3):1155–1162.
10. Howe D, Shannon JG, Winfree S, Dorward DW, Heinzen RA (2010) *Coxiella burnetii* phase I and II variants replicate with similar kinetics in degradative phagolysosome-like compartments of human macrophages. *Infect Immun* 78(8):3465–3474.
11. Hackstadt T, Williams JC (1981) Biochemical stratagem for obligate parasitism of eukaryotic cells by *Coxiella burnetii*. *Proc Natl Acad Sci USA* 78(5):3240–3244.
12. Omsland A, et al. (2009) Host cell-free growth of the Q fever bacterium *Coxiella burnetii*. *Proc Natl Acad Sci USA* 106(11):4430–4434.
13. Galán JE (2009) Common themes in the design and function of bacterial effectors. *Cell Host Microbe* 5(6):571–579.
14. Voth DE, Heinzen RA (2009) *Coxiella* type IV secretion and cellular microbiology. *Curr Opin Microbiol* 12(1):74–80.
15. Beare PA, Larson CL, Gilk SD, Heinzen RA (2012) Two systems for targeted gene deletion in *Coxiella burnetii*. *Appl Environ Microbiol* 78(13):4580–4589.
16. Beare PA, et al. (2011) Dot/Icm type IVB secretion system requirements for *Coxiella burnetii* growth in human macrophages. *MBio* 2(4):e00175–e11.
17. Carey KL, Newton HJ, Lührmann A, Roy CR (2011) The *Coxiella burnetii* Dot/Icm system delivers a unique repertoire of type IV effectors into host cells and is required for intracellular replication. *PLoS Pathog* 7(5):e1002056.
18. Chen C, et al. (2010) Large-scale identification and translocation of type IV secretion substrates by *Coxiella burnetii*. *Proc Natl Acad Sci USA* 107(50):21755–21760.
19. Lifshitz Z, et al. (2013) Computational modeling and experimental validation of the *Legionella* and *Coxiella* virulence-related type-IVB secretion signal. *Proc Natl Acad Sci USA* 110(8):E707–E715.
20. Lührmann A, Nogueira CV, Carey KL, Roy CR (2010) Inhibition of pathogen-induced apoptosis by a *Coxiella burnetii* type IV effector protein. *Proc Natl Acad Sci USA* 107(44):18997–19001.
21. Pan X, Lührmann A, Satoh A, Laskowski-Arce MA, Roy CR (2008) Ankyrin repeat proteins comprise a diverse family of bacterial type IV effectors. *Science* 320(5883):1651–1654.
22. Voth DE, et al. (2011) The *Coxiella burnetii* cryptic plasmid is enriched in genes encoding type IV secretion system substrates. *J Bacteriol* 193(7):1493–1503.
23. Voth DE, et al. (2009) The *Coxiella burnetii* ankyrin repeat domain-containing protein family is heterogeneous, with C-terminal truncations that influence Dot/Icm-mediated secretion. *J Bacteriol* 191(13):4232–4242.
24. Klingenbeck L, Eckart RA, Berens C, Lührmann A (2012) The *Coxiella burnetii* type IV secretion system substrate CaeB inhibits intrinsic apoptosis at the mitochondrial level. *Cell Microbiol* 15:675–687.
25. McDonough JA, et al. (2013) Host pathways important for *Coxiella burnetii* infection revealed by genome-wide RNA interference screening. *MBio* 4(1):e00606–e00612.
26. Berón W, Gutierrez MG, Rabinovitch M, Colombo MI (2002) *Coxiella burnetii* localizes in a Rab7-labeled compartment with autophagic characteristics. *Infect Immun* 70(10):5816–5821.
27. Gutierrez MG, et al. (2005) Autophagy induction favours the generation and maturation of the *Coxiella*-replicative vacuoles. *Cell Microbiol* 7(7):981–993.
28. Ghigo E, Colombo MI, Heinzen RA (2012) The *Coxiella burnetii* parasitophorous vacuole. *Adv Exp Med Biol* 984:141–169.

29. Bonifacino JS, Traub LM (2003) Signals for sorting of transmembrane proteins to endosomes and lysosomes. *Annu Rev Biochem* 72:395–447.
30. Canagarajah BJ, Ren X, Bonifacino JS, Hurley JH (2013) The clathrin adaptor complexes as a paradigm for membrane-associated allostery. *Protein Sci* 22(5):517–529.
31. Dinkel H, et al. (2012) ELM: The database of eukaryotic linear motifs. *Nucleic Acids Res* 40(Database issue):D242–D251.
32. Braulke T, Bonifacino JS (2009) Sorting of lysosomal proteins. *Biochim Biophys Acta* 1793(4):605–614.
33. Saftig P, Klumperman J (2009) Lysosome biogenesis and lysosomal membrane proteins: Trafficking meets function. *Nat Rev Mol Cell Biol* 10(9):623–635.
34. Beare PA, et al. (2009) Comparative genomics reveal extensive transposon-mediated genomic plasticity and diversity among potential effector proteins within the genus *Coxiella*. *Infect Immun* 77(2):642–656.
35. Huang L, et al. (2011) The E Block motif is associated with *Legionella pneumophila* translocated substrates. *Cell Microbiol* 13(2):227–245.
36. Zusman T, et al. (2007) The response regulator PmrA is a major regulator of the *icm/dot* type IV secretion system in *Legionella pneumophila* and *Coxiella burnetii*. *Mol Microbiol* 63(5):1508–1523.
37. Huotari J, Helenius A (2011) Endosome maturation. *EMBO J* 30(17):3481–3500.
38. Maxfield FR, McGraw TE (2004) Endocytic recycling. *Nat Rev Mol Cell Biol* 5(2): 121–132.
39. Lippincott-Schwartz J, et al. (1991) Brefeldin A's effects on endosomes, lysosomes, and the TGN suggest a general mechanism for regulating organelle structure and membrane traffic. *Cell* 67(3):601–616.
40. Ullrich O, Reinsch S, Urbé S, Zerial M, Parton RG (1996) Rab11 regulates recycling through the pericentriolar recycling endosome. *J Cell Biol* 135(4):913–924.
41. Dong X, et al. (2005) AP-3 directs the intracellular trafficking of HIV-1 Gag and plays a key role in particle assembly. *Cell* 120(5):663–674.
42. Doray B, Kornfeld S (2001) Gamma subunit of the AP-1 adaptor complex binds clathrin: Implications for cooperative binding in coated vesicle assembly. *Mol Biol Cell* 12(7):1925–1935.
43. Keyel PA, et al. (2006) A single common portal for clathrin-mediated endocytosis of distinct cargo governed by cargo-selective adaptors. *Mol Biol Cell* 17(10):4300–4317.
44. Kirchhausen T (1999) Adaptors for clathrin-mediated traffic. *Annu Rev Cell Dev Biol* 15:705–732.
45. Bonifacino JS, Lippincott-Schwartz J (2003) Coat proteins: Shaping membrane transport. *Nat Rev Mol Cell Biol* 4(5):409–414.
46. Bonifacino JS, Rojas R (2006) Retrograde transport from endosomes to the *trans*-Golgi network. *Nat Rev Mol Cell Biol* 7(8):568–579.
47. Mardones GA, et al. (2013) Structural basis for the recognition of tyrosine-based sorting signals by the μ3A subunit of the AP-3 adaptor complex. *J Biol Chem* 288(13): 9563–9571.
48. Mattera R, Boehm M, Chaudhuri R, Prabhu Y, Bonifacino JS (2011) Conservation and diversification of dileucine signal recognition by adaptor protein (AP) complex variants. *J Biol Chem* 286(3):2022–2030.
49. Sandoval IV, Martinez-Arca S, Valdueza J, Palacios S, Holman GD (2000) Distinct reading of different structural determinants modulates the dileucine-mediated transport steps of the lysosomal membrane protein LIMPII and the insulin-sensitive glucose transporter GLUT4. *J Biol Chem* 275(51):39874–39885.
50. Craig HM, Pandori MW, Guatelli JC (1998) Interaction of HIV-1 Nef with the cellular dileucine-based sorting pathway is required for CD4 down-regulation and optimal viral infectivity. *Proc Natl Acad Sci USA* 95(19):11229–11234.
51. Darsow T, Burd CG, Emr SD (1998) Acidic di-leucine motif essential for AP-3-dependent sorting and restriction of the functional specificity of the Vam3p vacuolar t-SNARE. *J Cell Biol* 142(4):913–922.
52. Janvier K, Bonifacino JS (2005) Role of the endocytic machinery in the sorting of lysosome-associated membrane proteins. *Mol Biol Cell* 16(9):4231–4242.
53. Schmidt U, et al. (2006) Endocytosis of the glucose transporter GLUT8 is mediated by interaction of a dileucine motif with the beta2-adaptin subunit of the AP-2 adaptor complex. *J Cell Sci* 119(Pt 11):2321–2331.
54. Doray B, Lee I, Knisely J, Bu G, Kornfeld S (2007) The gamma/sigma1 and alpha/sigma2 hemicomplexes of clathrin adaptors AP-1 and AP-2 harbor the dileucine recognition site. *Mol Biol Cell* 18(5):1887–1896.
55. Rodionov DG, et al. (2002) Structural requirements for interactions between leucine-sorting signals and clathrin-associated adaptor protein complex AP3. *J Biol Chem* 277(49):47436–47443.
56. Shih W, Gallusser A, Kirchhausen T (1995) A clathrin-binding site in the hinge of the beta 2 chain of mammalian AP-2 complexes. *J Biol Chem* 270(52):31083–31090.
57. Keyel PA, et al. (2008) The AP-2 adaptor beta2 appendage scaffolds alternate cargo endocytosis. *Mol Biol Cell* 19(12):5309–5326.
58. Janvier K, et al. (2003) Recognition of dileucine-based sorting signals from HIV-1 Nef and LIMP-II by the AP-1 gamma-sigma1 and AP-3 delta-sigma3 hemicomplexes. *J Cell Biol* 163(6):1281–1290.
59. Ren M, et al. (1998) Hydrolysis of GTP on rab11 is required for the direct delivery of transferrin from the pericentriolar recycling compartment to the cell surface but not from sorting endosomes. *Proc Natl Acad Sci USA* 95(11):6187–6192.
60. Wilcke M, et al. (2000) Rab11 regulates the compartmentalization of early endosomes required for efficient transport from early endosomes to the trans-golgi network. *J Cell Biol* 151(6):1207–1220.
61. Motley A, Bright NA, Seaman MN, Robinson MS (2003) Clathrin-mediated endocytosis in AP-2-depleted cells. *J Cell Biol* 162(5):909–918.
62. Dugast M, Toussaint H, Dousset C, Benaroch P (2005) AP2 clathrin adaptor complex, but not AP1, controls the access of the major histocompatibility complex (MHC) class II to endosomes. *J Biol Chem* 280(20):19656–19664.
63. Greenberg M, DeTulleo L, Rapoport I, Skowronski J, Kirchhausen T (1998) A dileucine motif in HIV-1 Nef is essential for sorting into clathrin-coated pits and for down-regulation of CD4. *Curr Biol* 8(22):1239–1242.
64. McCormick PJ, Martina JA, Bonifacino JS (2005) Involvement of clathrin and AP-2 in the trafficking of MHC class II molecules to antigen-processing compartments. *Proc Natl Acad Sci USA* 102(22):7910–7915.
65. Pornillos O, et al. (2003) HIV Gag mimics the Tsg101-recruiting activity of the human Hrs protein. *J Cell Biol* 162(3):425–434.
66. Punta M, et al. (2012) The Pfam protein families database. *Nucleic Acids Res* 40(Database issue):D290–D301.
67. Gilk SD, et al. (2013) Bacterial colonization of host cells in the absence of cholesterol. *PLoS Pathog* 9(1):e1003107.
68. Doray B, Knisely JM, Wartman L, Bu G, Kornfeld S (2008) Identification of acidic dileucine signals in LRP9 that interact with both GGAs and AP-1/AP-2. *Traffic* 9(9): 1551–1562.